Clinical Utility of Dual-Energy CT for Evaluation of Tophaceous Gout[1]

Madhura A. Desai, MD, PhD • Jeffrey J. Peterson, MD • Hillary Warren Garner, MD • Mark J. Kransdorf, MD

Although diagnosing gout generally is straightforward, atypical disease may present a challenge if it is associated with unusual symptoms or sites, discordant serum urate level, or mimics of gout. Dual-energy computed tomography (CT) may be used to differentiate urate crystals from calcium by using specific attenuation characteristics, which may help diagnose gout. In patients with known tophaceous gout, dual-energy CT may be used for serial volumetric quantification of subclinical tophi to evaluate response to treatment. Given the utility of dual-energy CT in challenging cases and its ability to provide an objective outcomes measure in patients with tophaceous gout, dual-energy CT promises to be a unique and clinically relevant modality in the diagnosis and management of gout.

ONLINE-ONLY CME

See www.rsna.org/education/rg_cme.html

LEARNING OBJECTIVES

After completing this journal-based CME activity, participants will be able to:

- Describe the basic technique of dual-energy CT.
- Identify the role of dual-energy CT in diagnosing gout.
- Discuss how dual-energy CT improves tophus quantification compared with other clinical or imaging techniques.

INVITED COMMENTARY

See discussion on this article by Nicolaou (pp 1376–1377).

TEACHING POINTS

See last page

Abbreviation: 3D = three-dimensional

RadioGraphics 2011; 31:1365–1375 • **Published online** 10.1148/rg.315115510 • **Content Codes:** CT MK

[1]From the Department of Radiology, Mayo Clinic Florida, 4500 San Pablo Rd, Jacksonville, FL 32224. Recipient of a Magna Cum Laude award for an education exhibit at the 2010 RSNA Annual Meeting. Received February 3, 2011; revision requested March 2 and received May 10; final version accepted May 23. For this journal-based CME activity, the authors, editor, and reviewers have no relevant relationships to disclose. **Address correspondence to** M.A.D. (e-mail: *mdgole@gmail.com*).

Introduction

Gout is characterized by the inflammatory response that results from the deposition of monosodium urate crystals in soft tissues and joints. Crystal deposition may lead to acute or chronic arthropathy and the formation of gouty tophi, nodular masslike aggregates of urate crystals (1). Gout is the most common crystalline type of arthropathy in the United States, and its incidence and prevalence continue to increase (2). Establishing a diagnosis of gout on the basis of clinical and laboratory criteria is generally straightforward. However, numerous cases have been described with atypical manifestations, which may obscure or delay clinical diagnosis and affect patient treatment (3). With the inherent capabilities of dual-energy computed tomography (CT), it is possible to distinguish urate from calcific mineralization, and dual-energy CT may be used in patients with an unclear diagnosis or in excluding gout. In patients with confirmed gout, when quantification of tophi is the desired outcome, it is important to compare the ability of dual-energy CT to perform volumetric analysis with that of other commonly used techniques. In this article, we discuss dual-energy CT techniques, present several cases in which the use of dual-energy CT helped establish a challenging clinical diagnosis, and demonstrate the ability of dual-energy CT to objectively quantify gouty tophus.

Dual-Energy CT

In dual-energy CT, two x-ray tubes with different peak kilovoltages (80 and 140 kVp) are used to simultaneously acquire two sets of images of the desired anatomic region (Fig 1). Materials act differently at different energies, depending on the elements of which they are composed (4). Comparing the material-specific differences in attenuation on the 80- and 140-kVp acquisitions allows differentiation of the chemical compositions of scanned tissues (5). Dual-energy CT has been used to successfully differentiate renal stones that contain uric acid from those that contain calcium or other materials (6–10), and the utility of this technique has been extrapolated for its use in depicting gout. Dual-energy CT may be used to differentiate uric acid from calcium in musculoskeletal tissue, allowing gouty urate crystals to be distinguished from bone or dystrophic calcifications (Fig 2).

Teaching Point

The ability of dual-energy CT to differentiate between uric acid and calcium is highly advantageous compared with radiography and routine diagnostic CT, at which urate crystals and calcium-containing mineralizations often demonstrate indistinguishable high attenuation. Furthermore, the simultaneous acquisitions in dual-energy CT eliminate misregistration artifacts and reduce errors due to patient movement. Postprocessing of dual-energy CT data yields color-coded cross-sectional images. In addition, three-dimensional (3D) surface-rendered models may be produced and viewed 360° around any axis; these simple and elegant models are ideal for conveying tophus burden and location to both clinicians and patients (Fig 3).

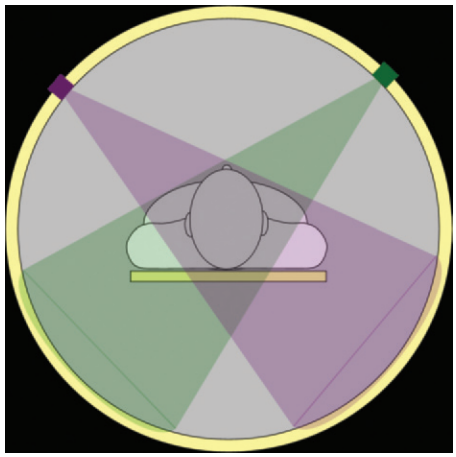

Figure 1. Diagram shows the dual acquisitions that are used in dual-energy CT, in which 80- and 140-kVp x-ray tubes simultaneously acquire data, a process that reduces error from misregistration or patient movement.

Challenging Diagnoses

The gold standard for establishing a diagnosis of gout is to determine whether monosodium urate crystals are present in aspirated joint fluid or tophus. However, samples of joint fluid frequently are not obtained; in these cases, disease manifestation, serum urate levels, and radiologic findings are key to establishing a clinical diagnosis of gout (11,12). Several criteria for diagnosis have been developed over the years, including hyperuricemia, the presence of tophi or urate crystals, acute onset of painful monoarthropathy (especially at the first metatarsophalangeal joint), response to colchicine, and radiologic findings (13,14). With these criteria, diagnosing gout generally is straightforward; however, it may be challenging in several settings, such as in patients with an unusual clinical presentation (eg, abnormal site, prolonged rate of onset, or polyarthropathy), an acute gouty attack with normal serum urate levels, an active attack (rather than a chronic sequela of disease), and hyperuricemia with an inflammatory disease that imitates gout.

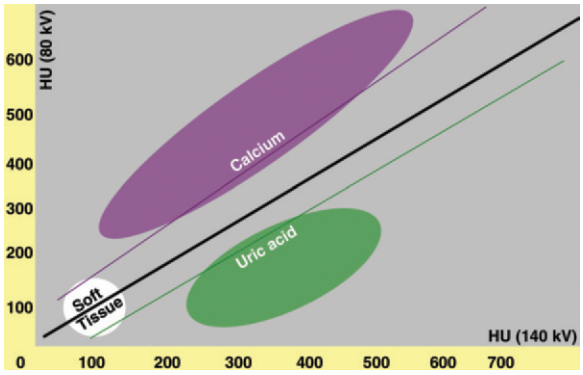

Figure 2. Graph shows how composition of tissues is determined. Material-specific differences in attenuation (measured in HU and not to scale) between the 80- and 140-kV acquisitions help determine chemical composition of scanned tissues.

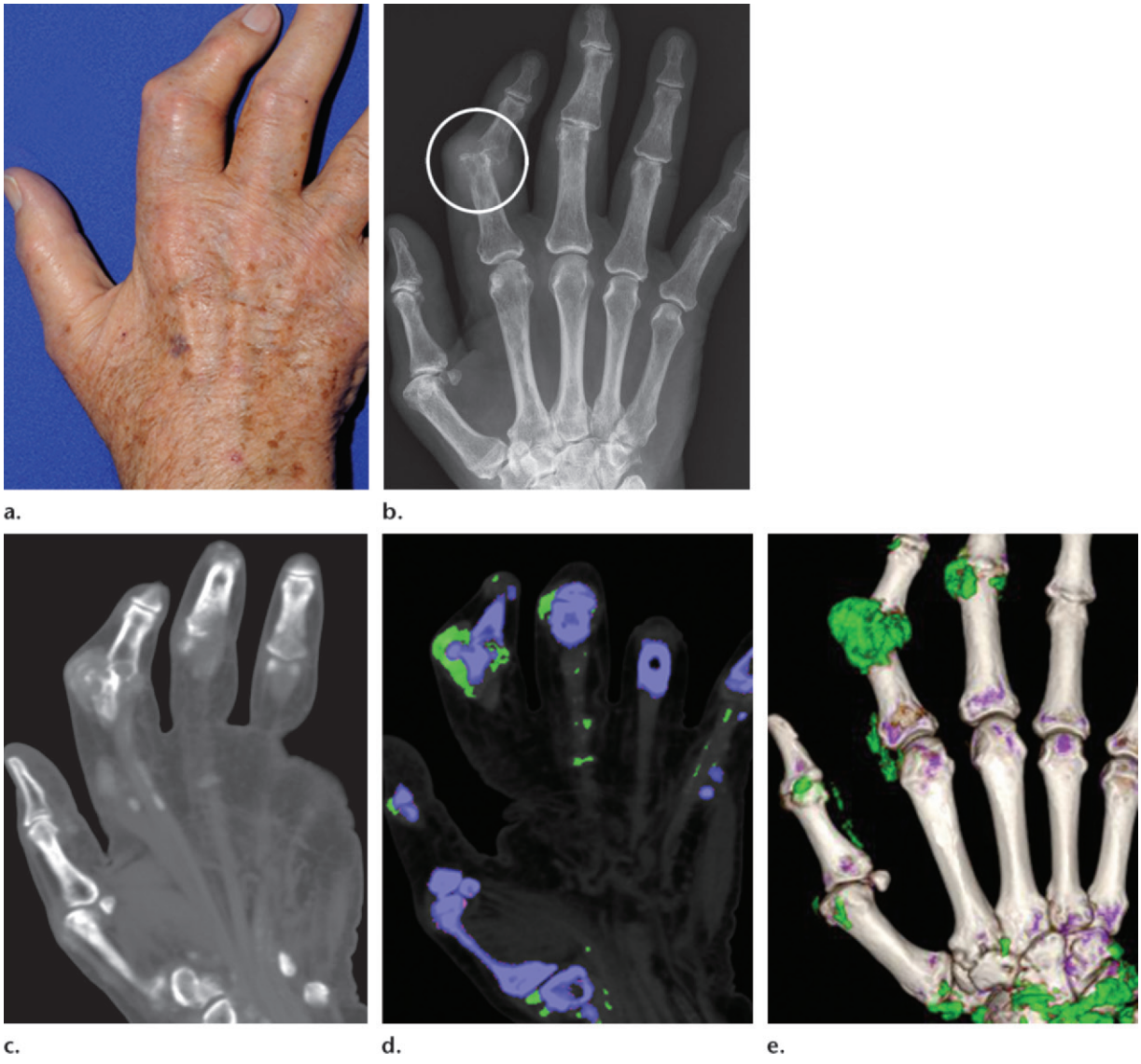

Figure 3. Known tophaceous gout. **(a)** Photograph obtained at clinical examination of an index finger shows soft-tissue swelling and deformity of the proximal interphalangeal joint. **(b)** Anteroposterior radiograph shows mineralized tophus and classic periarticular "rat bite" erosions (circle) at the proximal interphalangeal joint of the index finger. **(c, d)** Diagnostic CT **(c)** and color-coded composition CT **(d)** images obtained with postprocessing techniques by using data from dual-energy CT show uric acid deposits (green areas in **d**) within the tophus and at additional clinically occult sites. These uric acid deposits are distinct from calcium-containing osseous structures (blue areas in **d**). **(e)** Surface-rendered 3D CT image obtained with further postprocessing shows the anatomic relationship between the uric acid–containing tophi (green areas) and osseous structures (white and purple areas).

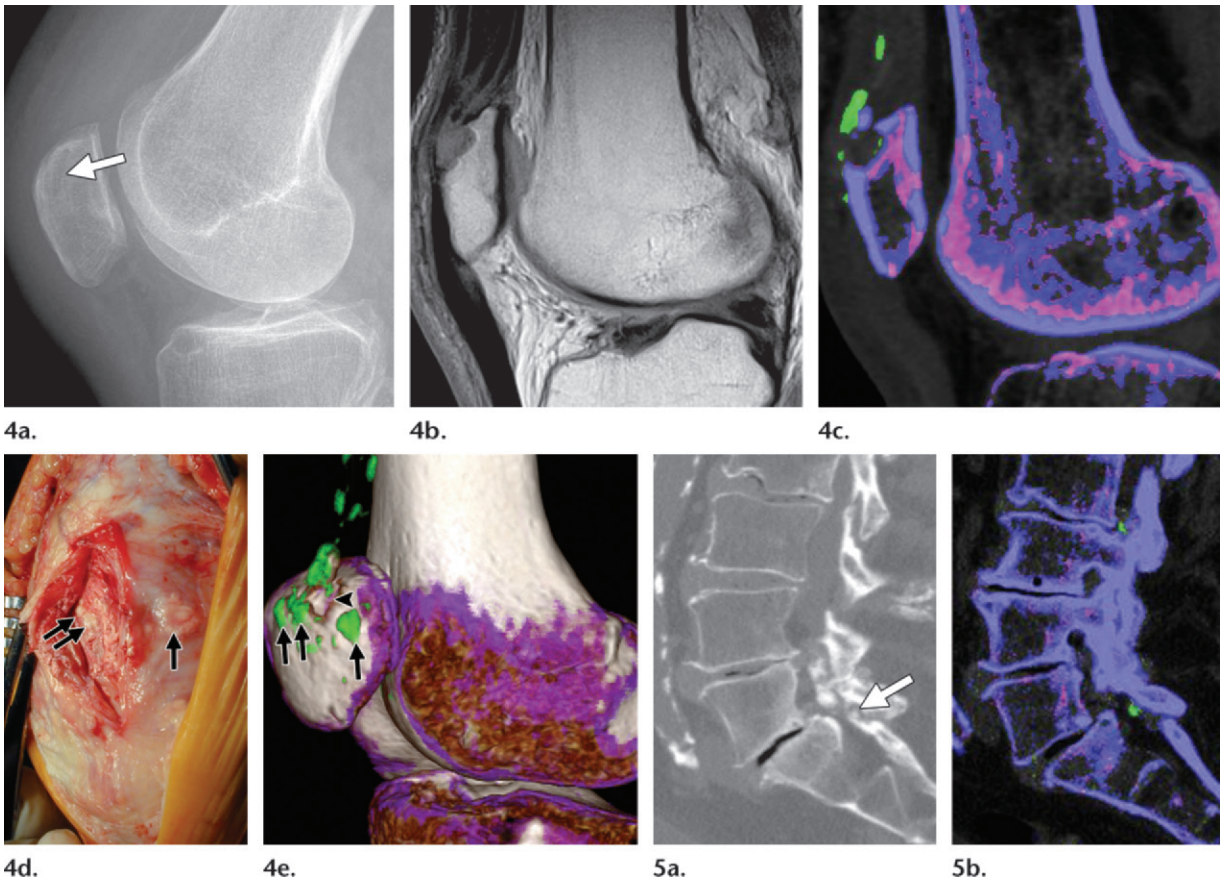

Figures 4, 5. **(4)** Patellar gout in an 87-year-old man with anterior knee pain, elevated serum uric acid level, no pain in any other joints, and no history of gout. **(a)** Lateral radiograph shows a subtle lytic lesion in the upper pole of the patella (arrow). **(b)** Sagittal fast spin-echo proton-density–weighted magnetic resonance (MR) image shows nonspecific intermediate-signal-intensity soft tissue within the patellar lytic lesion, a finding that does not exclude malignancy, and an area of abnormal signal intensity within and around the thickened distal quadriceps tendon, a finding consistent with tendinosis. **(c)** Sagittal color-coded dual-energy CT image shows urate deposition (green areas) in the periphery of the lytic lesion, a finding consistent with gouty erosion. Urate deposition also is seen along the quadriceps tendon. **(d)** Intraoperative photograph (anterolateral oblique view) shows gross urate deposition (arrows) along the quadriceps tendon and overlying the patella. **(e)** Anterolateral 3D CT image, in oblique projection, shows the lytic patellar lesion (arrowhead). Arrows = urate deposition. **(5)** Lumbar facet joint gout in an 82-year-old man with worsening lower back pain and a longstanding history of hyperuricemia and tophaceous gout in the extremities. The patient received minimal relief from multiple facet joint injections. **(a)** Sagittal CT image shows spondylosis of the lower lumbar spine, with disk space narrowing and "vacuum phenomenon" at L4-5 and L5-S1 and advanced facet degenerative changes. A small area of erosion with mineralization also is seen at the right L5-S1 facet (arrow). **(b)** Sagittal color-coded dual-energy CT image shows a small focus of urate (green area) at the right L5-S1 facet joint, a finding that corresponds to the area of erosion seen at CT and is consistent with gout. The patient's medical history revealed that his lumbar symptoms worsened after colchicine therapy was discontinued because of toxicity.

Unusual Clinical Manifestation

In the most common clinical manifestation of acute gout, rapid onset of a painful monoarthopathy occurs in the distal appendicular skeleton, often in the first metatarsophalangeal joint (podagra), in a middle-aged man or a postmenopausal woman. Atypical clinical manifestations also are seen with increased frequency in certain segments of the population, including the elderly and patients who underwent organ transplantation and those with a tumor, prostheses, and genetic mutations (3). Gout with an atypical manifestation may be mistaken for malignancy or infection. It also may initially be overlooked if it is in an unusual location, such as the proximal appendicular or axial skeleton, or in patients who initially present with polyarthropathy (Fig 4–6). In such cases, dual-energy CT provides a quick, noninvasive way to identify deposition of monosodium urate crystals and establish a diagnosis of gout, which may reduce unnecessary delays in diagnosis and minimize morbidity resulting from misdiagnosis (15).

Discordant Serum Urate Levels

As was previously mentioned, hyperuricemia is a common clinical criterion used in the diagnosis

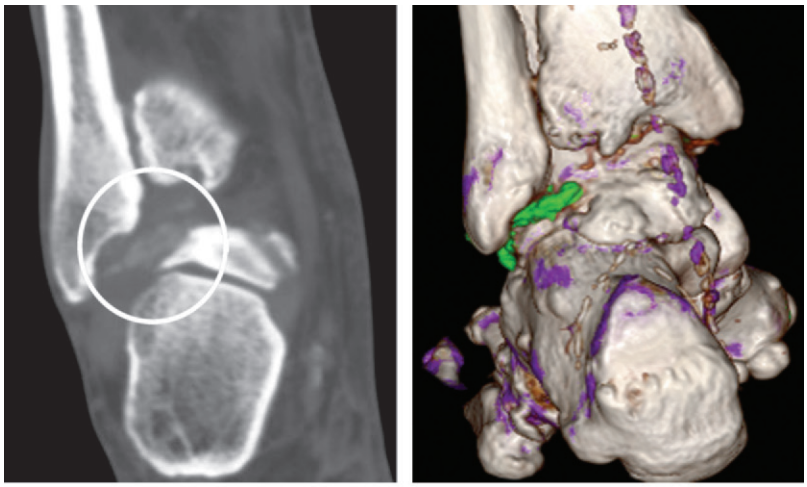

a. b.

Figure 6. Polyarthropathy in a 65-year-old man with normal serum urate level, normal serum uric acid level, and swelling and pain of bilateral wrists and ankles. Although rheumatoid arthritis was suspected, rheumatoid factor, anti–cyclic citrullinated peptide and antinuclear antibody test results were negative. The most symptomatic joint was imaged. **(a)** Coronal CT image shows ill-defined mineralization in the lateral aspect of the ankle mortise (circle). **(b)** Three-dimensional model, in posterior projection, shows the green urate deposits, a finding that helps establish a diagnosis of gouty arthritis.

7a. 7b. 8a. 8b.

Figures 7, 8. **(7)** Acute tophaceous gout in a 46-year-old man with normal serum urate level. The patient developed an acute episode of gout despite having taken the prescribed medications. **(a)** Posteroanterior radiograph shows vague mineralization surrounding the first metatarsophalangeal joint and the second proximal interphalangeal joint. **(b)** Three-dimensional model, in plantar projection, shows the mineralization, which corresponds to urate deposits (green areas) and is consistent with classic tophaceous gouty arthritis. **(8)** Active gout in a 62-year-old man with normal serum urate level and swelling and pain around the second digit. Although he had a remote history of gout, his serum uric acid level was normal. **(a)** Sagittal CT image shows that the second digit flexor tendon is thickened, contains mineralization, and is surrounded by inflammatory changes. **(b)** Sagittal color-coded dual-energy CT image shows green urate crystal deposits along the flexor tendon, a finding consistent with gout-related tendinopathy.

of gout. Serum urate levels higher than 404.5 μmol/L (6.8 mg/dL) are above that of saturation and may lead to precipitation and deposition of urate crystals into joints and soft tissues (11). The normal range varies among laboratories, but usually there is an upper range of normal that is above the level of urate saturation; thus, deposition may be seen even at so-called normal urate levels, and acute gouty attacks may occur in patients with normal serum urate levels (16–18). Although hyperuricemia is the predominant risk factor for gout, elevated serum urate levels do not always lead to deposition of urate crystals (19).

In patients with gout, serum levels vary with time and treatment, which may result in a continuously shifting balance that leads to deposition of crystals or resuspension or resorption. Because dual-energy CT may directly depict urate crystal deposition, it is specifically used to evaluate for gout regardless of patients' serum urate levels. Thus, dual-energy CT findings may easily confirm a diagnosis of gout in patients with normal serum urate levels or exclude it in patients with hyperuricemia (Figs 7, 8) (20).

Teaching Point

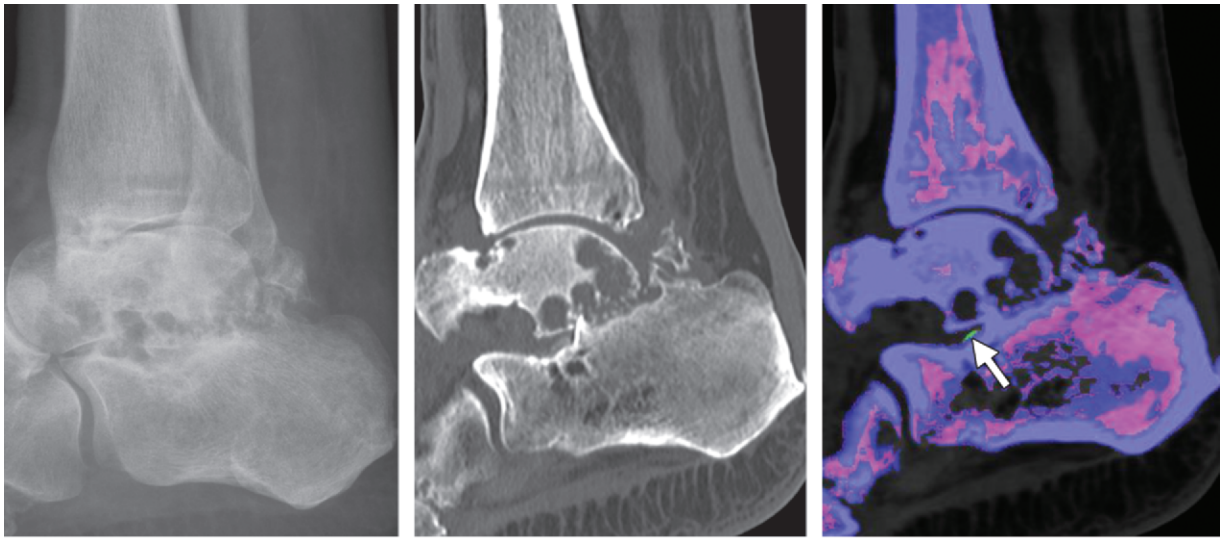

a. b. c.

Figure 9. Small component of active gout in a 62-year-old man with normal serum urate level, normal serum uric acid level, a remote history of gout, and ankle pain and effusion. **(a)** Lateral radiograph of the ankle shows advanced erosive or cystic changes, as well as degenerative changes, in the subtalar joint. **(b)** Sagittal CT image better shows the erosive changes seen at radiography. Several small areas of associated mineralization also are seen. **(c)** Color-coded dual-energy CT image shows only a small focus of urate crystal deposition within the subtalar joint (arrow). The remainder of the erosive change represents sequelae of remote gouty attacks.

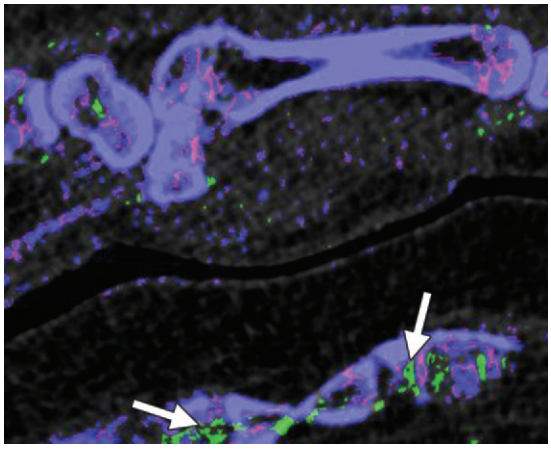

Figure 10. Asymptomatic costochondral gout in a 76-year-old man with rapid onset of polyarticular arthropathy and a normal serum uric acid level. Because of limitations in positioning, the patient's hand and wrist were imaged on top of his chest. Sagittal color-coded dual-energy CT image of the hand and wrist shows tiny diffuse green foci of urate crystal deposition, a finding consistent with gout. Because of the way the patient is positioned, the asymptomatic costochondral joints were incidentally imaged deep to the hand and also demonstrate urate crystal deposition (arrows).

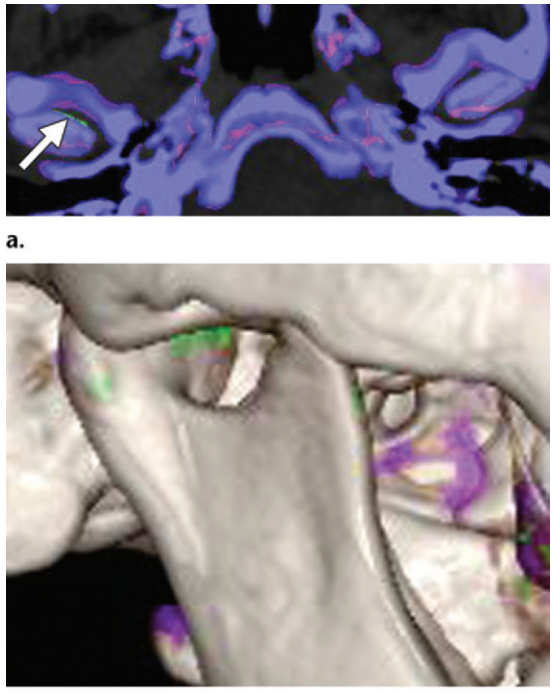

a. b.

Figure 11. Asymptomatic temporomandibular joint gout in a 63-year-old woman with a family history of gout and pain in the cervical spine. **(a)** Color-coded dual-energy CT image shows asymmetric deposition of urate crystals in the right temporomandibular joint (arrow), which was asymptomatic. No gouty involvement was seen in the cervical spine. **(b)** Three-dimensional model, in anterolateral projection, shows deposition of urate crystals in the right temporomandibular joint.

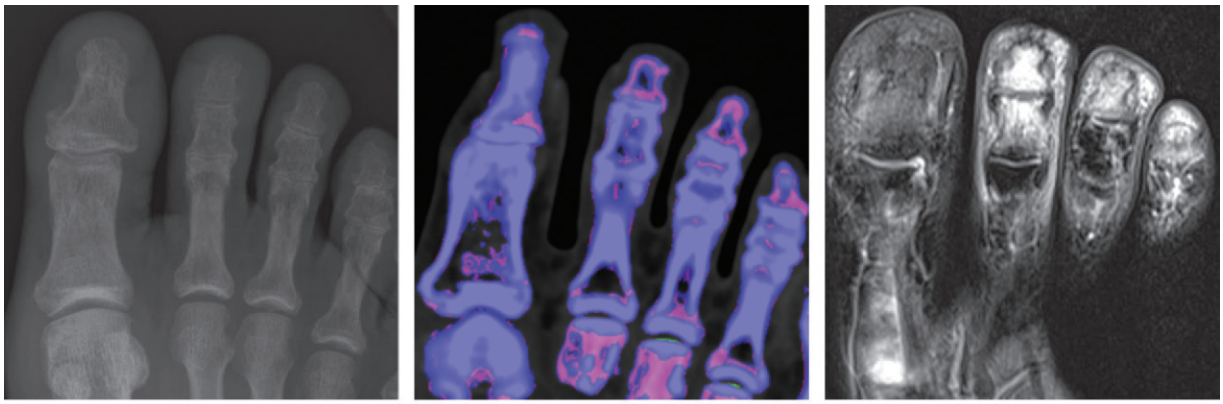

a. b. c.

Figure 12. Osteomyelitis in a 64-year-old man with a known history of gout, swelling and pain in the second right toe, and borderline high serum uric acid level. A new gouty attack was suspected. **(a)** Radiograph of the forefoot shows soft-tissue swelling involving the second toe, with no osseous abnormalities. **(b)** Dual-energy CT image shows no urate crystal deposition, a finding that excludes gout. **(c)** Long-axis T2-weighted fast spin-echo MR image shows an area of abnormal signal intensity in the bone marrow and soft tissue of the distal second toe, a finding consistent with osteomyelitis. Osteomyelitis was confirmed at indium-111–labeled white blood cell scintigraphy (not shown).

Acute and Chronic Changes

Dual-energy CT may be used to correlate crystal deposition with osseous changes. Classic osseous radiographic findings include well-defined "punched out" periarticular erosions with overhanging edges, normal mineralization, relative preservation of the joint spaces, and asymmetric distribution that eventually becomes polyarticular. After an acute attack, classic osseous findings take several years to manifest, so if these findings are seen with no urate crystal deposition, they may be due to remote, currently inactive gout, and alternative causes for acute-onset arthropathy may be pursued (Fig 9) (21). It has been suggested that the simultaneous presence of osseous findings and urate crystals is indicative of active gout superimposed with chronic gouty change.

Teaching Point

Subclinical Disease

Monosodium urate crystals have been detected in aspirates from asymptomatic joints in which there is no inflammation. Despite the lack of clinical features, the presence of urate crystals is considered diagnostic of gout (22,23). Similarly, dual-energy CT may depict subclinical urate crystal deposition at other asymptomatic sites that have been included in the imaging field, which helps establish a diagnosis of gout and enables initiation of treatment before irreversible joint damage occurs (Figs 10, 11) (24). In asymptomatic patients, identification of urate crystals also may lead to earlier recognition and treatment of underlying hyperuricemia, a condition that has been associated with increased cardiovascular risk and metabolic syndrome (25–30).

Teaching Point

Mimics of Gout

Septic arthritis and osteomyelitis (Fig 12), pseudogout (calcium pyrophosphate deposition disease), and rheumatoid arthritis are common mimics of gout (31). Less often, malignancy, other arthritides (Fig 13), and tendinopathy (Fig 14) also may clinically imitate gout. Because of their overlapping symptoms and laboratory markers, inflammatory processes may be difficult to distinguish clinically, and they may be even more challenging to differentiate in

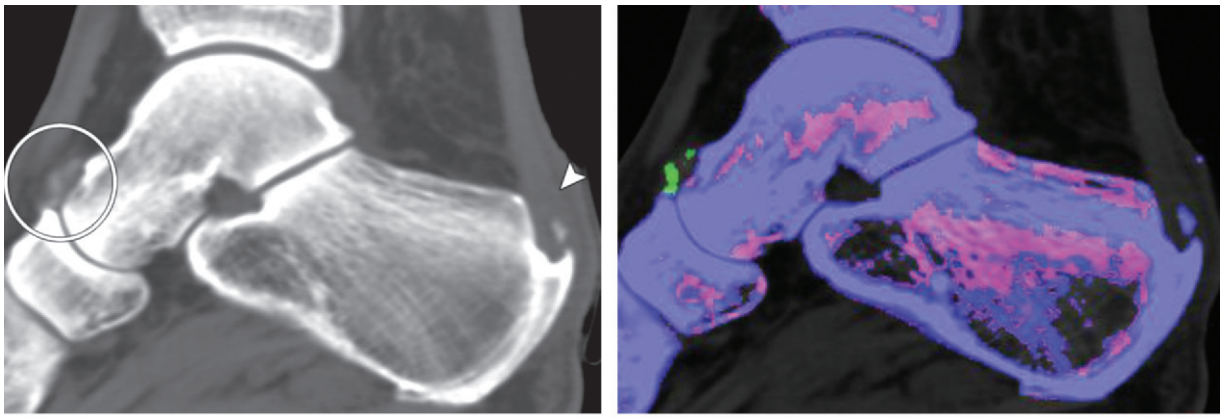

a. b.

Figure 13. Tendinopathy in a 70-year-old man with hyperuricemia, a history of podagra, and acute pain and swelling posterior to the heel. Gouty involvement was suspected. **(a)** Sagittal CT image shows abnormal thickening of the Achilles tendon (arrowhead), a finding consistent with tendinosis. Ill-defined mineralization also is seen at the dorsal aspect of the talonavicular joint (circle). **(b)** Sagittal color-coded dual-energy CT image shows no urate crystal deposition in the region of the distal Achilles tendon, a finding that excludes gout-related tendinopathy. Here, the distal Achilles tendon mineralization seen at CT is actually part of the calcium-containing calcaneal spur. However, the green mineralization at the dorsal talonavicular joint does represent urate crystal deposition, a finding indicative of tophaceous gout in unsuspected nearby areas.

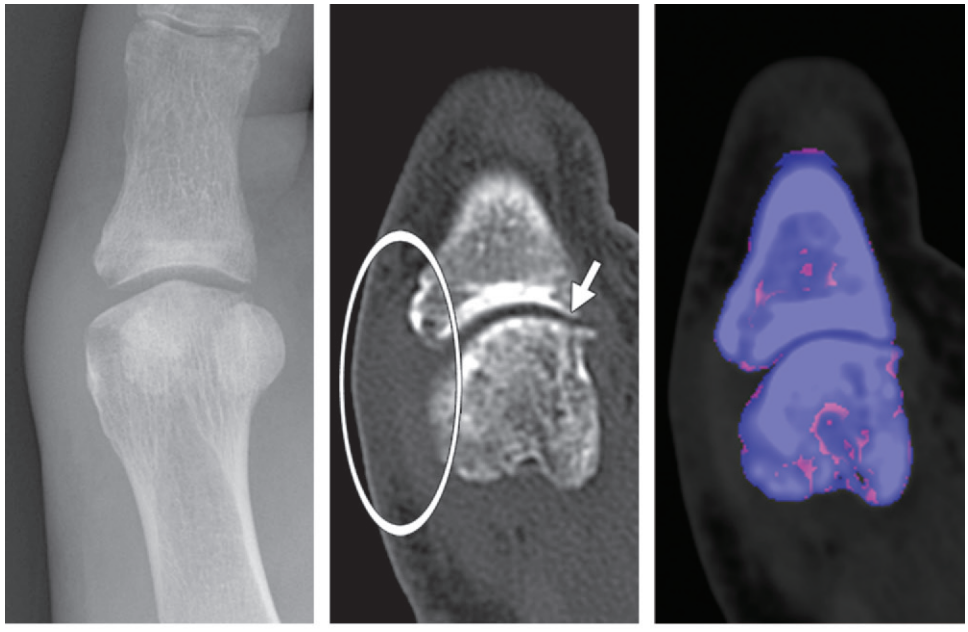

a. b. c.

Figure 14. Osteoarthritis in a 52-year-old man with hyperuricemia, a history of tophaceous gout, and pain and swelling of the first metatarsophalangeal joint. Acute gout recurrence was suspected. **(a)** Radiograph shows subtle asymmetric soft-tissue swelling around the medial first metatarsophalangeal joint, with no evidence of erosion or mineralization. **(b)** Long-axis CT image shows soft-tissue swelling around the medial aspect of the first metatarsophalangeal joint (oval), with mild medial joint space narrowing (arrow) and early osteophyte formation. **(c)** Color-coded dual-energy CT image shows no urate crystal deposition, a finding that excludes gout. These findings are most consistent with osteoarthritis.

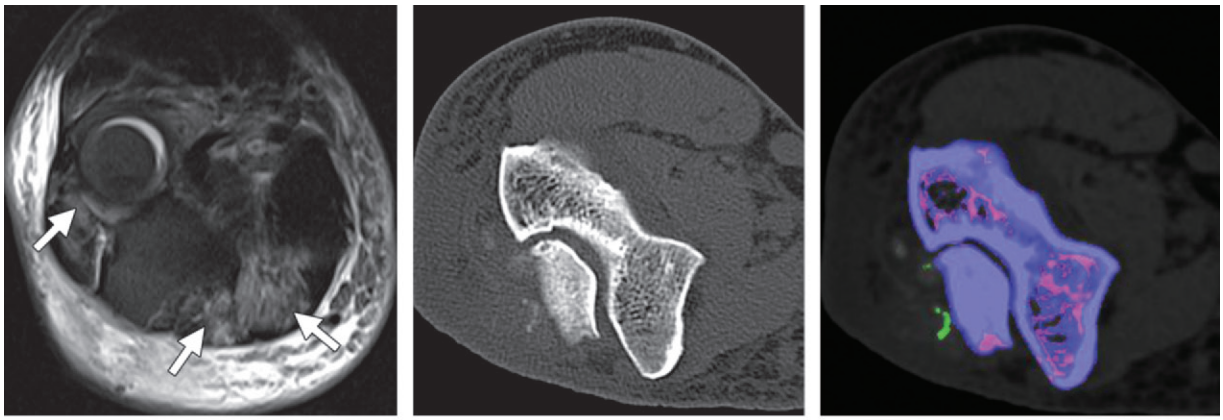

Figure 15. Concurrent gout with myositis and cellulitis in a 63-year-old man with a history of gout, normal serum uric acid level, elevated white blood cell count, marked soft-tissue swelling, and pain around the elbow. Septic arthritis was suspected, but no joint fluid could be aspirated. **(a)** Axial T2-weighted fat-saturated fast spin-echo MR image shows extensive subcutaneous edema around the posterior elbow, with abnormal signal intensity within the musculature of the extensor and posterior flexor compartments (arrows) at the level of the radial head, findings that are consistent with cellulitis and myositis. **(b)** CT image shows several foci of mineralization around the posterior elbow. **(c)** At color-coded dual-energy CT, the foci of mineralization are found to contain urate crystals, a finding consistent with gout. Although either gout or cellulitis alone could have produced the patient's symptoms, the combination of dual-energy CT and MR imaging helped establish a diagnosis of concurrent gout and myositis with cellulitis. The patient began antibiotic and antigout therapy, with a presumably better response than if he had been treated for a single disease process.

patients with hyperuricemia or known gout elsewhere in the body. In such cases, dual-energy CT findings may be valuable in excluding urate crystal deposition, and they have been shown to help distinguish gout from inflammatory mimics such as psoriasis, rheumatoid arthritis, pseudogout, and pigmented villonodular synovitis (24). In addition, if the degree of inflammatory change seems out of proportion to the amount of crystal deposition identified at dual-energy CT, a concurrent disease process may need to be considered in addition to gout (Fig 15).

Quantification of Gouty Tophus

In patients with chronic gout, quantification of tophi and documentation of regression are important monitoring measures, with the ultimate goal to prevent joint destruction (32). Common methods of evaluation include clinical assessment (counting the number of tophi and measuring them with a tape measure or calipers), radiography, ultrasonography (US), CT, and MR imaging. Clinical measurements are limited to tophi that are subcutaneously visible or palpable and do not reflect the entire tophus burden. In addition, reproducibility may be affected by factors such as anatomic location, size, and observer experience (33). Although late osseous findings are well-depicted at radiography, tophi are not always visible, and if they are, their margins may be difficult to delineate and evaluate for interval change (21). Conventional CT and MR imaging have improved sensitivity and specificity for detection and quantification of tophi; however, both modalities require that users manually delineate tophus margins for volumetric calculations (34–36). US is able to depict both subcutaneous and intraarticular tophi, but it is operator-dependant, and tophus measurements usually are limited to a few index lesions (37). Unlike these modalities, dual-energy CT is inherently able to distinguish urate crystal deposits from surrounding structures, and it provides sensitive and specific volumetric quantification with no user variability (5). The overall tophus burden or volume of uric acid deposition may be calculated for individual lesions, joints, or the entire scanned area. Its ability to quantify tophi without significant user variability makes dual-energy CT an ideal tool for evaluating even small changes in tophus burden, and it may be used to document response to treatment for purposes of daily practice or clinical trials (Fig 16) (38).

Teaching Point

a. b.

Figure 16. Determination of change in tophus burden at serial dual-energy CT. Images were obtained 6 weeks apart. Visually, the changes in tophus burden are difficult to compare because of differences in positioning and the small amount of change present. Serial dual-energy CT images with volumetric analysis show a tophus burden with a volume of 10.78 cm^3 **(a)** and 9.95 cm^3 **(b)**, findings that represent an 8.3% decrease in tophus burden, a change that corresponds to medical treatment and an interval drop in serum urate level, from 624.6 to 493.7 μmol/L (10.5 to 8.3 mg/dL).

Summary

A diagnosis of gout is generally straightforward and is usually reached by evaluating clinical, laboratory, and radiologic findings. By using specific attenuation characteristics to differentiate urate crystals from calcium, dual-energy CT may be helpful when the diagnosis is unclear, as in cases of atypical clinical manifestations, discordant levels of serum urate, or in differentiating an acute attack from chronic changes. Dual-energy CT also helps exclude gout in patients with inflammatory mimics, regardless of serum urate level or history of gout. In patients with known tophaceous gout, dual-energy CT may depict subclinical tophi so that treatment may be initiated before irreversible joint damage occurs, and it provides sensitive and specific volumetric quantification of tophi without significant user variability. Moreover, dual-energy CT provides a way to share tophus burden with clinicians and patients in an elegant and simple 3D model. Because of its utility in challenging cases and its ability to provide an objective outcomes measure in patients with tophaceous gout, dual-energy CT promises to be a unique and clinically relevant modality for the diagnosis and management of gout.

References

1. Richette P, Bardin T. Gout. Lancet 2010;375(9711):318–328.
2. Lawrence RC, Felson DT, Helmick CG, et al. Estimates of the prevalence of arthritis and other rheumatic conditions in the United States. Part II. Arthritis Rheum 2008;58(1):26–35.
3. Ning TC, Keenan RT. Unusual clinical presentations of gout. Curr Opin Rheumatol 2010;22(2):181–187.

4. Coursey CA, Nelson RC, Boll DT, et al. Dual-energy multidetector CT: how does it work, what can it tell us, and when can we use it in abdominopelvic imaging? RadioGraphics 2010;30(4):1037–1055.
5. Karcaaltincaba M, Aktas A. Dual-energy CT revisited with multidetector CT: review of principles and clinical applications. Diagn Interv Radiol 2010 Nov 14. [Epub ahead of print]
6. Primak AN, Fletcher JG, Vrtiska TJ, et al. Noninvasive differentiation of uric acid versus non-uric acid kidney stones using dual-energy CT. Acad Radiol 2007;14(12):1441–1447.
7. Graser A, Johnson TR, Bader M, et al. Dual energy CT characterization of urinary calculi: initial in vitro and clinical experience. Invest Radiol 2008;43(2):112–119.
8. Ascenti G, Siragusa C, Racchiusa S, et al. Stone-targeted dual-energy CT: a new diagnostic approach to urinary calculosis. AJR Am J Roentgenol 2010;195(4):953–958.
9. Stolzmann P, Kozomara M, Chuck N, et al. In vivo identification of uric acid stones with dual-energy CT: diagnostic performance evaluation in patients. Abdom Imaging 2010;35(5):629–635.
10. Hidas G, Eliahou R, Duvdevani M, et al. Determination of renal stone composition with dual-energy CT: in vivo analysis and comparison with x-ray diffraction. Radiology 2010;257(2):394–401.
11. Schlesinger N. Diagnosis of gout: clinical, laboratory, and radiologic findings. Am J Manag Care 2005;11(15 Suppl):S443–S450; quiz S465–S468.
12. Chen LX, Schumacher HR. Gout: can we create an evidence-based systematic approach to diagnosis and management? Best Pract Res Clin Rheumatol 2006;20(4):673–684.
13. Wallace SL, Robinson H, Masi AT, Decker JL, McCarty DJ, Yü TF. Preliminary criteria for the classification of the acute arthritis of primary gout. Arthritis Rheum 1977;20(3):895–900.
14. Zhang W, Doherty M, Pascual E, et al. EULAR evidence based recommendations for gout. Part I. Diagnosis: report of a task force of the Standing Committee for International Clinical Studies Including Therapeutics (ESCISIT). Ann Rheum Dis 2006;65(10):1301–1311.
15. Johnson TR, Weckbach S, Kellner H, Reiser MF, Becker CR. Clinical image: Dual-energy computed tomographic molecular imaging of gout. Arthritis Rheum 2007;56(8):2809.
16. McCarty DJ. Gout without hyperuricemia. JAMA 1994;271(4):302–303.
17. Logan JA, Morrison E, McGill PE. Serum uric acid in acute gout. Ann Rheum Dis 1997;56(11):696–697.
18. Schlesinger N, Baker DG, Schumacher HR Jr. Serum urate during bouts of acute gouty arthritis. J Rheumatol 1997;24(11):2265–2266.
19. Roddy E, Doherty M. Epidemiology of gout. Arthritis Res Ther 2010;12(6):223.
20. Nicolaou S, Yong-Hing CJ, Galea-Soler S, Hou DJ, Louis L, Munk P. Dual-energy CT as a potential new diagnostic tool in the management of gout in the acute setting. AJR Am J Roentgenol 2010;194(4):1072–1078.
21. Buckley TJ. Radiologic features of gout. Am Fam Physician 1996;54(4):1232–1238.
22. Agudelo CA, Weinberger A, Schumacher HR, Turner R, Molina J. Definitive diagnosis of gout by identification of urate crystals in asymptomatic metatarsophalangeal joints. Arthritis Rheum 1979;22(5):559–560.
23. Bomalaski JS, Lluberas G, Schumacher HR Jr. Monosodium urate crystals in the knee joints of patients with asymptomatic nontophaceous gout. Arthritis Rheum 1986;29(12):1480–1484.
24. Choi HK, Al-Arfaj AM, Eftekhari A, et al. Dual energy computed tomography in tophaceous gout. Ann Rheum Dis 2009;68(10):1609–1612.
25. Baker JF, Krishnan E, Chen L, Schumacher HR. Serum uric acid and cardiovascular disease: recent developments, and where do they leave us? Am J Med 2005;118(8):816–826.
26. Choi HK, Curhan G. Independent impact of gout on mortality and risk for coronary heart disease. Circulation 2007;116(8):894–900.
27. Feig DI, Kang DH, Johnson RJ. Uric acid and cardiovascular risk. N Engl J Med 2008;359(17):1811–1821.
28. Krishnan E. Gout and coronary artery disease: epidemiologic clues. Curr Rheumatol Rep 2008;10(3):249–255.
29. Puig JG, Martínez MA. Hyperuricemia, gout and the metabolic syndrome. Curr Opin Rheumatol 2008;20(2):187–191.
30. Dao HH, Harun-Or-Rashid M, Sakamoto J. Body composition and metabolic syndrome in patients with primary gout in Vietnam. Rheumatology (Oxford) 2010;49(12):2400–2407.
31. Sack K. Monarthritis: differential diagnosis. Am J Med 1997;102(1A):30S–34S.
32. Grainger R, Taylor WJ, Dalbeth N, et al. Progress in measurement instruments for acute and chronic gout studies. J Rheumatol 2009;36(10):2346–2355.
33. Dalbeth N, Schauer C, Macdonald P, et al. Methods of tophus assessment in clinical trials of chronic gout: a systematic literature review and pictorial reference guide. Ann Rheum Dis 2011;70(4):597–604.
34. Dalbeth N, Clark B, Gregory K, Gamble GD, Doyle A, McQueen FM. Computed tomography measurement of tophus volume: comparison with physical measurement. Arthritis Rheum 2007;57(3):461–465.
35. Schumacher HR Jr, Becker MA, Edwards NL, et al. Magnetic resonance imaging in the quantitative assessment of gouty tophi. Int J Clin Pract 2006;60(4):408–414.
36. Popp JD, Bidgood WD Jr, Edwards NL. Magnetic resonance imaging of tophaceous gout in the hands and wrists. Semin Arthritis Rheum 1996;25(4):282–289.
37. Thiele RG. Role of ultrasound and other advanced imaging in the diagnosis and management of gout. Curr Rheumatol Rep 2011;13(2):146–153.
38. Bacani AK, McCollough CH, Glazebrook KN, et al. Dual energy computed tomography for quantification of tissue urate deposits in tophaceous gout: help from modern physics in the management of an ancient disease. Rheumatol Int 2009 Dec 17. [Epub ahead of print]

Clinical Utility of Dual-Energy CT for Evaluation of Tophaceous Gout[1]

Madhura A. Desai, MD, PhD • Jeffrey J. Peterson, MD • Hillary Warren Garner, MD • Mark J. Kransdorf, MD

RadioGraphics 2011; 31:1365–1375 • **Published online** 10.1148/rg.315115510 • **Content Codes:** CT MK

Page 1366
Comparing the material-specific differences in attenuation on the 80- and 140-kVp acquisitions allows differentiation of the chemical compositions of scanned tissues (5).

Page 1369 (Figures on page 1369)
Because dual-energy CT may directly depict urate crystal deposition, it is specifically used to evaluate for gout regardless of patients' serum urate levels. Thus, dual-energy CT findings may easily confirm a diagnosis of gout in patients with normal serum urate levels or exclude it in patients with hyperuricemia (Figs 7, 8) (20).

Page 1371 (Figure on page 1370)
After an acute attack, classic osseous findings take several years to manifest, so if these findings are seen with no urate crystal deposition, they may be due to remote, currently inactive gout, and alternative causes for acute-onset arthropathy may be pursued (Fig 9) (21).

Page 1371 (Figures on page 1370)
Similarly, dual-energy CT may depict subclinical urate crystal deposition at other asymptomatic sites that have been included in the imaging field, which helps establish a diagnosis of gout and enables initiation of treatment before irreversible joint damage occurs (Figs 10, 11) (24).

Page 1373 (Figure on page 1374)
The overall tophus burden or volume of uric acid deposition may be calculated for individual lesions, joints, or the entire scanned area. Its ability to quantify tophi without significant user variability makes dual-energy CT an ideal tool for evaluating even small changes in tophus burden, and it may be used to document response to treatment for purposes of daily practice or clinical trials (Fig 16) (38).